E-symmetry phonon polaritons in $PbTiO_3$

J. C. Loulergue* and J. Etchepare
Laboratoire d'Optique Appliquée, Ecole Nationale Supérieure de Techniques Avancées, Ecole Polytechnique, Centre National de la Recherche Scientifique URA 1406, Centre de l'Yvette, 91120 Palaiseau, France
(Received 17 April 1995; revised manuscript received 10 July 1995)

We have measured the dispersion of the two lowest E-symmetry phonon polariton branches in $PbTiO_3$ for wave-vector values up to 3000 cm^{-1}. The time domain transient grating experimental scheme used is well suited to state that at room temperature no pure relaxation motion, specifically from an order-disorder crystal, can be evidenced. Nevertheless, the polariton dispersion behavior can only be explained by a model which takes into account a weak relaxational mode with an ill-defined origin. This behavior, deduced from a fit to the static dielectric constant, is characteristic of the mixed mechanism for ferroelectricity in $PbTiO_3$, as in a lot of other perovskites.

I. INTRODUCTION

Lead titanate is known as a nominally pure ferroelectric crystal which undergoes a displacive type structural phase transition. Nevertheless, recent works suggested that some order-disorder character has to be taken into account. Sicron *et al.*[1] showed from an x-ray absorption fine-structure analysis that an essential element of order-disorder is present in the cubic phase of $PbTiO_3$, a fact which corroborates findings by Fontana *et al.*[2] on the existence of a central peak near the transition temperature. It has been also demonstrated by a Raman analysis of quasimodes[3] that the pioneer's Burns and Scott[4] attributions had to be revised, that would consequently lead to a crossing at elevated temperature of the lowest frequency A_1 and E soft modes.

As a matter of fact, the processes involved in phase transitions of solids can be addressed by an exhaustive study of phonon characteristics. In fact, the behavior as a function of temperature of the phonon frequency and damping has been extensively studied in the past using Raman spectroscopy as a primary tool. It has been recently demonstrated that nonlinear spectroscopy methods, with the use of ultrashort temporal laser pulses, allow direct excitation of low frequency vibrational modes through the so-called impulsive stimulated Raman scattering (ISRS) process.[5–7] This technique is particularly relevant, as the modes which are of primary concern are in the low frequency regime. Moreover, a forward four-wave mixing scheme, which enables the excitation of phonons at small wave-vector values, is of specific interest in the case of polar modes as it allows an easy description of the phonon-polariton dispersion[8] and therefore a determination of each mode contribution to the overall dielectric constant. At least, a time resolved experiment may give new insight into the nature of the phase transition mechanisms as the displacive and order-disorder characters have drastically different signatures in the time domain.[9–11]

Previously published work[12] showed that the A_1 symmetry component to the phase transition in $PbTiO_3$ is displacive in nature, and is adequately described by the lowest frequency soft mode. The case of E modes is of special interest, as several authors[13] using Raman experiments conclude the presence of a resonance in the damping of polaritons centered at 40 cm^{-1}, a frequency well above the minimum value which can be achieved in our apparatus. We present in this article results on the E-symmetry part of the low frequency phonon polariton dispersion at room temperature. Excitation of nonsymmetric modes, although inherently identical to that of symmetric ones, has only been reported previously, to our knowledge, by Dougherty *et al.*[14] We will therefore first discuss specifically these excitations and demonstrate that in $PbTiO_3$ two of the three E modes are accessible by our femtosecond pulses. The essential purpose of the present work is therefore to describe the dispersion of these two lowest phonon-polariton modes, as a function of wave-vector values from $cq/2\pi \approx 200$ cm^{-1} up to ≈ 3000 cm^{-1}. This will allow us to deduce their contribution to the static dielectric constant. The information obtained will form a basis for a future temperature dependent study, close to the ferroelectric phase transition at 766 K.

II. GEOMETRICAL CONSIDERATIONS

A four wave mixing experiment in a forward arrangement leads to the excitation of phonon(s) of wave vector q, whose value is related directly to the angle between the pump beams by the relation $q=(2 \sin \theta/2)/\lambda$, where θ is the angle between the pump beams external to the crystal. This simple case corresponds to a completely symmetric arrangement, in which pump pulse polarizations are parallel to each other. This configuration is well suited for the excitation of symmetric motions. In order to drive E-symmetry modes in $PbTiO_3$ crystal, one can choose perpendicular polarizations for the pump beams, along y and z crystal axis, whereas the beams are propagating in the x direction (Fig. 1). This provides access to the c coefficient of the Raman polarizability tensor, whereas the induced polarization is along the y axis. We are in this case concerned with a true TO mode.

The problem of definition of the q vector is less trivial than for the symmetric arrangement, as the two beams propagate along directions with different indices, namely n_0 and n_e. Nevertheless, an exact definition of the q value is important, as we want to study the q-dependent behavior of the phonon polaritons. The q vector can be described by two components $q_\parallel$ and $q_\perp$, parallel and perpendicular to the di-

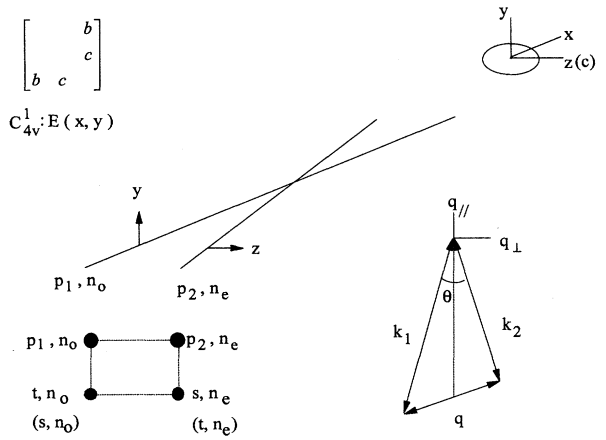

FIG. 1. Geometrical considerations: p_1, p_2, s, and t correspond to the propagation directions of the two pump beams, the signal, and the probe beam; n_0 and n_e stand for the polarization directions of the beams. The lower right part allows one to define $q_\parallel$ and $q_\perp$ components. Upper right part gives the $PbTiO_3$ refractive index ellipse in the yz plane and upper left part recalls the Raman tensor elements of E symmetry and the direction of the induced polarization.

rection of propagation of the beam respectively. They are given by

$$q_\perp = 2/\lambda \sin(\theta/2) \tag{1a}$$

$$q_\parallel = 1/\lambda[(n_0^2 - \sin^2(\theta/2))^{1/2} - (n_e^2 - \sin^2(\theta/2))^{1/2}] \tag{1b}$$

As a matter of fact, a more general formulation has to be built up[15] for the $q_\parallel$ component to take into account the variation of the refractive indices as a function of the wavelength concerned to drive a specific phonon of frequency Ω. The $q_\parallel$ component is a function of three parameters: λ any wavelength value inside the pump frequency spectral width, Ω the phonon frequency, and θ the angle between the pump beams. Integration over λ leads to a spread in the wave vector values, resulting in a lowering of the diffraction efficiency as a function of q, and giving rise to an intrinsic damping of the resultant mean polariton frequency. Modification of q values as a function of driven phonon frequencies Ω are insignificant for the cases we present hereafter; the various polaritons, which can be driven at the same θ value, have therefore the same wave vector. However, in the case of $PbTiO_3$, an exact calculation of q values using the formulation given in Ref. 15 leads to results which differ from those obtained using (1a) and (1b) by amounts on the order of the accuracy of the measurement of the angle θ. As the phonon wave-vector direction is no more perpendicular to the mean pump beam propagation direction, the phase matching conditions for the overall process is realized (in a Bragg configuration) only when the polarization direction of the probe beam is properly chosen (insert of Fig. 1).

Excitation of two counterpropagating waves leads to the creation of a stationary wave, and the signal is therefore proportional to the square of the induced polarization change. The general form of the time dependent signal can be written as

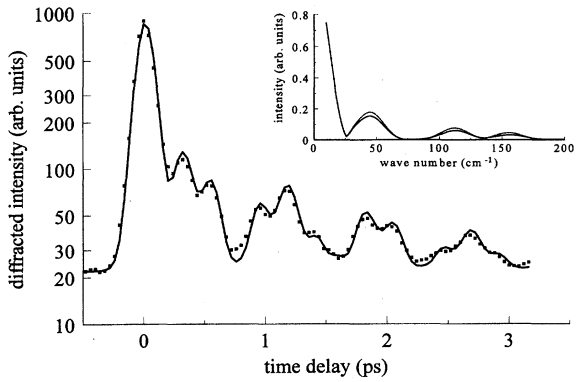

FIG. 2. Diffraction efficiency of the transient grating as a function of time delay between pump and probe pulses in a semilogarithmic scale. Squares correspond to experimental results and the continuous curve to the numerical fit. The upper part corresponds to experimental (continuous) and theoretical (dashed) Fourier transforms of the results.

$$S(t) \propto \left[A \exp(-t/\tau) + \sum_{i=1,2} A_i \exp(-t/\tau_i) \sin(\omega_i t + \varphi_i) \right]^2 . \tag{2}$$

In this expression, we have *a priori* taken into account uncoupled contributions from a relaxational motion and from two damped oscillatory modes. In a nonresonant regime, the phase factors would be equal to zero. For clarity, the electronic contribution to the signal and the convolution products due to the finite sizes of the pump and probe temporal pulses have been omitted from Eq. (2). A prime advantage of a quadratic dependence of the signal is easier detection of a pure relaxation process, which would be the signature of an order-disorder contribution. Indeed, if the impulse response function of the material is only made of two oscillators with frequencies ω_1 and ω_2, the Fourier transform of the signal will ideally contain four peaks at frequencies $2\omega_1$, $2\omega_2$, $\omega_2-\omega_1$, and $\omega_2+\omega_1$. Existence of a strong relaxational process, with a characteristic time in the same range as the damping of the oscillators, will lead to the appearance of two other peaks at frequencies ω_1 and ω_2 (Ref. 16). One of the disadvantages of this interference effect is the increased complication of the signal analysis than for a linear dependence.

III. EXPERIMENTAL RESULTS

The laser system used in this experiment is a colliding pulse mode locked dye laser, connected to an amplifier which delivers pulses at a repetition rate of 20 Hz. The pulse temporal width is 80 fs, the energy for each pump beam incident on the crystal is several μJ, and the central wavelength of 620 nm. The single crystal used[17] has a thickness of 0.3 mm along the a axis.

Figure 2 shows the experimental results obtained for an angle $\theta/2 = 0.246°$, which corresponds to $q = 217\ cm^{-1}$, the lowest wave-vector value available with our setup. The complicated temporal response is the signature of several interfering frequencies. A Fourier transform (FT) calculation of the temporal signal gives several peaks. Their number and

TABLE I. Frequencies obtained by Fourier transform of the signal and their attributions to polariton modes, with regard to $\theta/2$ angle between pump beams and corresponding q values.

$\theta/2$ (deg)	q (cm^{-1})	ν_a (cm^{-1})	ν_b (cm^{-1})	ν_c (cm^{-1})	ν_1 (cm^{-1})	ν_2 (cm^{-1})
0.246	217	42.2 ($2\nu_1$)	111.6 ($\nu_2-\nu_1$)	155.4 ($\nu_2+\nu_1$)	21.8	133.5
0.281	230	49.1 ($2\nu_1$)	110.0 ($\nu_2-\nu_1$)	157.9 ($\nu_2+\nu_1$)	24.6	134.0
0.344	256	50.6 ($2\nu_1$)	109.4 ($\nu_2-\nu_1$)	161.0 ($\nu_2+\nu_1$)	25.8	135.2
0.398	280	58.5 ($2\nu_1$)	106.9 ($\nu_2-\nu_1$)	165.2 ($\nu_2+\nu_1$)	29.2	136.4
0.514	334	66.3 ($2\nu_1$)	103.2 ($\nu_2-\nu_1$)	170.4 ($\nu_2+\nu_1$)	33.1	136.7
0.611	383	74.1 ($2\nu_1$)	98.5 ($\nu_2-\nu_1$)		37.1	135.5
0.840	502	94.4 ($2\nu_1$)	94.4 ($\nu_2-\nu_1$)	189.1 ($\nu_2+\nu_1$)	47.2	141.9
0.884	526	92.2 ($\nu_2-\nu_1$)	97.5 ($2\nu_1$)	193.0 ($\nu_2+\nu_1$)	49.5	142.5
1.007	591	90.7 ($\nu_2-\nu_1$)	104.7 ($2\nu_1$)	195.0 ($\nu_2+\nu_1$)	52.4	142.8
1.051	615	89.1 ($\nu_2-\nu_1$)	107.8 ($2\nu_1$)		53.9	143.0
1.066	623	88.2 ($\nu_2-\nu_1$)	112.5 ($2\nu_1$)	200.0 ($\nu_2+\nu_1$)	55.9	144.2
1.205	698	90.7 ($\nu_2-\nu_1$)	119.0 ($2\nu_1$)	209.0 ($\nu_2+\nu_1$)	59.1	149.8
1.260	729	89.1 ($\nu_2-\nu_1$)	121.0 ($2\nu_1$)	211.0 ($\nu_2+\nu_1$)	60.5	150.2
1.320	762	89.0 ($\nu_2-\nu_1$)	126.0 ($2\nu_1$)	215.0 ($\nu_2+\nu_1$)	63.0	152.0
1.460	839	88.9 ($\nu_2-\nu_1$)	132.7 ($2\nu_1$)	221.6 ($\nu_2+\nu_1$)	66.3	155.3
1.590	911	88.1 ($\nu_2-\nu_1$)	138.1 ($2\nu_1$)	226.0 ($\nu_2+\nu_1$)	69.0	157.0
1.676	958	91.3 ($\nu_2-\nu_1$)	142.9 ($2\nu_1$)	232.0 ($\nu_2+\nu_1$)	71.4	162.7
2.021	1150	90.7 ($\nu_2-\nu_1$)	148.5 ($2\nu_1$)	239.1 ($\nu_2+\nu_1$)	74.5	164.8
2.215	1258	96.0 ($\nu_2-\nu_1$)	153.8 ($2\nu_1$)	249.1 ($\nu_2+\nu_1$)	76.5	172.0
3.040	1719	103.2 ($\nu_2-\nu_1$)	164.1 ($2\nu_1$)	267.3 ($\nu_2+\nu_1$)	82.1	185.2
3.668	2070	107.8 ($\nu_2-\nu_1$)	167.2 ($2\nu_1$)		83.6	191.4
5.199	2928	115.7 ($\nu_2-\nu_1$)	170.4 ($2\nu_1$)		85.2	200.9

position is a function of angle θ. Table I presents the experimental results as a function of angle θ, with regard to q wave vectors whose values have been calculated using the refractive index measurements by Singh *et al.*[18] The peaks ν_a, ν_b, etc. obtained from Fourier transform analysis of the measured signals have been assigned to linear combination of eigenvalues ν_1 and ν_2. We can therefore deduce the values of the two lowest phonon-polariton wave numbers. Examination of Table I shows that none of the TF peaks has been attributed to a single frequency. This result leads to the conclusion that no purely relaxational process can describe the temporal behavior. We can therefore conclude that there is no direct feature which would imply the existence of an order-disorder behavior at room temperature. An exhaustive analysis of A_i, τ_i, and φ_i ($i=1,2$) values, as a function of q, which can be extracted from a fit of Eq. (2) to the experimental data will not be presented here. We only summarize the essential features.

(i) Damping of the two lowest polariton branches do not vary significantly over the explored q values range. Their dependency, as a function of q, is in fact inside the error bar corresponding to the accuracy of our fitting procedure. This seems surprising for the lowest branch, for which a continuous decrease of the damping would be expected when q tends toward zero value. This fact cannot be explained by the spread in q values, which leads to a maximum intrinsic damping value of about 1 cm^{-1}. We do not at the opposite recover Raman scattering experimental results,[13] where the damping was shown to increase, by a factor of 3, as q decreased and reached a maximum around 50 cm^{-1}. An explanation for these discrepancies with previously published trends may be attributed to limitations currently reached in spectral domain experiments, where one can hardly differentiate between spurious scattered light and true phonon-polariton scattering in a forward geometry. Our values, $\tau_1=(3.75\pm0.9)$ ps and $\tau_2=(1.6\pm0.4)$ ps, which correspond to full width at half maximum of $\gamma_1=(5\pm1)$ cm^{-1} and $\gamma_2=(11\pm2)$ cm^{-1} are in the range of those published for ω_{TO} frequencies.[2,20]

(ii) The phase lags φ_i do change drastically as a function of q values. If φ_i values are close to 0° for small q values (<600 cm^{-1}), they reach respectively $\varphi_1\approx30°$ and $\varphi_2\approx90°$ for q values >1000 cm^{-1}. We will discuss this particular point hereafter.

As we measured the phonon-polariton dispersion curve,

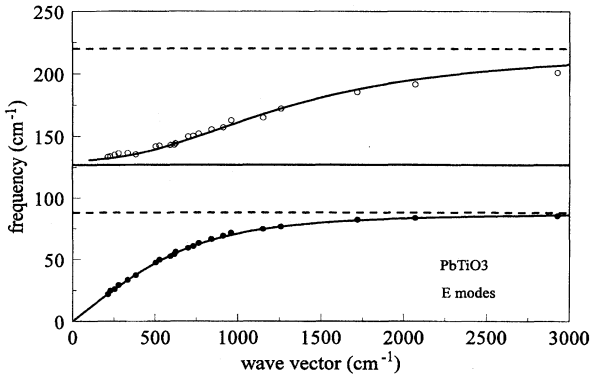

FIG. 3. Experimental points of E-symmetry polaritons in $PbTiO_3$ and theoretical dispersion curves obtained using parameters from Table II.

TABLE II. Experimental values of ω_{TO}, ω_{LO} frequencies, and γ_{TO} dampings. $(1+\Sigma S_j)$ values of columns 1 to 3 are obtained from generalized (Lyddane-Sachs-Teller) relation. S_j values of Refs. 4 and 20 are obtained from IR data. This work S_j values are the result of a fit from polariton dispersion curves: $S_{j,1}$ without any relaxational mode; $S_{j,2}$ with a relaxational coupling to the second polariton branch.

	Refs. 2,20				Ref. 1		Ref. 4			This work	
	ω_{TO} (cm^{-1})	γ_{TO} (cm^{-1})	ω_{LO} (cm^{-1})	S_j	ω_{TO}	ω_{LO}	ω_{TO}	ω_{LO}	S_i	$S_{j,1}$	$S_{j,2}$
	88	5	128.5	10.96	87.5	128	89	128	10.11	9.0	9.5
	220.2	12	440	5.48	218.5	440.5	221	445	5.37	4.0	5.2
	506	14	686	0.28	505	687	508	717	0.27	0.3	0.3
ΣS_j				16.72						13.3	15.0
$1+\Sigma S_j$		15.6				16.1		16.7		14.3	16.0

our results are very sensitive to the value of the static dielectric constant $\epsilon(0)$. Therefore, one of the parameters which can be accurately deduced from an analysis of the phonon-polariton dispersion is the contribution of each driven mode to the static dielectric constant. The simplest general form for the total dielectric constant $\epsilon(\Omega)$ at frequency Ω is given by the phenomenological expression

$$\epsilon(\Omega)=\epsilon(\infty)\left[1+\sum_j \frac{S_j\omega_{TOj}^2}{\Omega_{TOj}^2-\Omega^2-i\Omega\gamma_{TOj}}\right], \tag{3}$$

where $\epsilon(\infty)$ is the high frequency (optical) dielectric constant, and the contribution from each mode j at frequency ω_{TOj} is a function of its oscillator strength S_j and damping γ_j. This quantity is used to calculate the polariton response as stated by Barker and Loudon:[19]

$$R(q,\Omega)=\mathrm{Im}\left\{\frac{1}{c^2q^2/\Omega^2-\epsilon(\Omega)}\right\}. \tag{4}$$

The maxima of this function define the polariton dispersion. In the fitting procedure used to estimate S_j parameters, values for ω_{TO_1}, γ_{TO_1}, ω_{TO_2}, and γ_{TO_2} are taken from the literature.[2,3,20] The third branch cannot be reached in our experiment. Its contribution to the dielectric constant, which is known to be very small, was taken as a constant value, say S_3'. In Fig. 3 are plotted the frequency polariton values deduced from an analysis of the Fourier transform of the temporal response and the fitted curves. Resulting $S_{j,1}$ oscillator strengths are collected in Table II, with regard to several experimental data. Nevertheless, the static dielectric constant along a axis, $\epsilon_a=\epsilon(0)$, which is derived from (3) using $\epsilon(\infty)=6.36$, is 94.1, significantly smaller than the clamped experimental value $\epsilon_a^s=106.9$.

Since our setup is very sensitive to the polariton frequency dispersion, we have used the polariton behavior as a function of wave vector to have a better insight into the dielectric constant characteristics. Several parameters may be added, which would lead to a better description of $\epsilon(0)$. A first model consists in the addition of an infrared active relaxational mode, characterized by a strength S_r and a damping Γ_r. Another possibility is in incorporating only a coupling of the oscillator(s) with Debye relaxation(s),[21] where δ_j is the coupling strength to the j phonon branch and Γ_j is the associate relaxation-mode damping. In a general manner, the overall contribution to the dielectric constant can then be written as

$$\epsilon(\Omega)=\epsilon(\infty)\left[1+\sum_{j=1,2}\frac{S_j(\omega_{TO_j}^2-\delta_j^2)}{\omega_{TO_j}^2-\Omega^2-i\Omega\gamma_{TO_j}-\dfrac{\Gamma_j\delta_j^2}{\Gamma_j-i\Omega}}+S_3'+\frac{S_r}{1-i\Omega\Gamma_r}\right]. \tag{5}$$

The goal of the fit is to obtain values of the oscillators (and relaxator) strengths in concordance with the static dielectric constant: $\epsilon(0)=\epsilon(\infty)[1+\Sigma_i S_i+S_r]$. On one hand, it is trivial to see that $S_{j,1}$ parameters of Table I, to which is added an infrared active relaxation mode of strength $S_r=1.7$, will lead to an adequate description of $\epsilon(0)$. On another hand, a coupling process may also give a correct static dielectric constant value. In this case, we have seen that adjustment to the dispersion curves is very sensitive to δ_j values. The best fit is obtained for $\delta_1=0.0$ cm^{-1} and $\delta_2=100$ cm^{-1}. This estimated value of the coupling strength compares well with results obtained on $LiNbO_3$, by quasielastic light scattering.[22] In every case, the fit do not depend hardly on Γ. We only notice that its value is likely to be located in the pico- or subpicosecond range.[11,23]

Finally we should note[10] that Fourier transform of the spectral response connected to $\epsilon(\Omega)$ given by Eq. (5) gives a temporal domain signal strictly analogous to Eq. (2). Depending on the model used, parameters A and τ of the relaxational exponential term are either directly related to Γ_r and S_r or, in the case of a coupling, related to Γ_j and coupling strengths δ_j. As a matter of fact, it can be seen that A value is very small compared to A_i. Another argument in favor of a relaxational mode is the existence of phase terms in the

temporal response of the polaritons. We have seen that φ_i values obtained using Eq. (2) are significantly different from zero for values of $q > 1000$ cm^{-1}.

These findings differ from those obtained by Raman scattering where no central peak has been detected at room temperature. The explanation of this discrepancy may be attributed to the Brillouin zone range involved in respectively 90° Raman scattering experiments and forward measurements. They correspond, in real space, to correlation lengths which can differ by at least one order of magnitude.

IV. CONCLUSION

In this paper, we have presented the observation of coherent excitation of the two lowest phonon-polariton E modes in $PbTiO_3$, measured at room temperature in the temporal domain. Their behavior as a function of wave vector values up to $cq/2\pi \approx 3000$ cm^{-1} were analyzed in detail. The first result which can be deduced from this study is a direct consequence of the quadratic nature of the signal with respect to the transient induced nonlinear polarization. The assignment of none of the FT peaks to an eigenfrequency leads to the conclusion that no pure relaxation motion can be actually detected at room temperature.

A better insight into the problem of the structure of this perovskite has been obtained by an exhaustive study of the phonon polariton dispersion. The simplest model used to describe the static dielectric constant from a fit of the phonon oscillator strengths included contributions from two damped oscillators. It results in S_j values in disagreement with what can be deduced from the static dielectric constant value. From this discrepancy we can conclude that a relaxational mode is likely to be present but that this mode is so weak that it does not affect the measured temporal signals for the actual driven polaritons. This suggests the existence, even at room temperature, of different average and local distortions of the lattice, upon a correlation length characteristic of the q-wave-vector range explored.

An exhaustive study of relaxation times and phase factors associated to the polariton oscillators will hopefully allow to reinforce one of the advanced hypothesis on a Debye relaxation mechanism. It seems already that in perovskites, there is a general occurrence of a coupling effect rather than pure relaxation and/or oscillatory processes. Moreover the usual assertion, which claims that an order-disorder character is described by an exponential signal in the temporal domain, has to be considered carefully as we have seen that the existence of a temporal signal with a relaxational character can be due to either the existence of a weak Debye relaxator or the only signature of a tight coupling between an oscillator and a relaxator.

Study of the temperature dependent behavior of these two lowest E-symmetry polariton modes are in progress. This will give information on the possible strengthening of a hypothetic coupling or reveal a true relaxation motion close to the transition temperature toward the cubic phase of this perovskite.

ACKNOWLEDGMENTS

We wish to thank O. Albert, M. Duijser, and P. Zaparucha for their assistance in numerical analysis, P. Bourson and M. Fontana (Université de Metz and Supelec) for an exhaustive discussion of their published and unpublished works.

*Also at C.L.O.E.S. Université de Metz-Supelec, 2 rue Belin, 57078 Metz, France.

[1] N. Sicron, B. Ravel, Y. Yacoby, E. A. Stern, F. Dogan, and J. J. Rehr, Phys. Rev. B **50**, 13 168 (1994).

[2] M. D. Fontana, K. Wojcik, H. Idrissi, and G. E. Kugel, Ferroelectrics **107**, 91 (1990).

[3] C. M. Foster, Z. Li, M. Grimsditch, S. K. Chan, and D. J. Lam, Phys. Rev. B **48**, 10 160 (1993).

[4] G. Burns and B. A. Scott, Phys. Rev. B **7**, 3088 (1973).

[5] Y. Yan and K. A. Nelson, J. Chem. Phys. **87**, 6240 (1987).

[6] G. G. Cho, W. Kûtt, and H. Kurtz, Phys. Rev. Lett. **65**, 764 (1990).

[7] H. J. Zeiger, J. Vidal, T. K. Cheng, E. P. Ippen, and G. Dresselhaus, Phys. Rev. B **45**, 768 (1992).

[8] J. Etchepare, G. Grillon, A. Antonetti, J. C. Loulergue, M. D. Fontana, and G. Kugel, Phys. Rev. B **41**, 12 362 (1990).

[9] P. C. Planken, L. D. Noordam, J. T. M. Kennis, and A. Lagendijk, Phys. Rev. B **45**, 7106 (1992).

[10] P. Grenier, D. Houde, S. Jandl, and L. A. Boatner, Phys. Rev. B **47**, 1 (1993).

[11] H. J. Bakker, S. Hunsche, and H. Kurz, Phys. Rev. B **48**, 13 524 (1993).

[12] D. P. Kien, J. C. Loulergue, and J. Etchepare, Phys. Rev. B **47**, 11 027 (1993).

[13] D. Heiman and S. Ushioda, Phys. Rev. B **17**, 3616 (1978).

[14] T. P. Dougherty, G. P. Wiederrecht, K. A. Nelson, M. H. Garret, H. P. Jensen, and C. Ward, Science **258**, 770 (1992); T. P. Dougherty, G. P. Wiederrecht, and K. A. Nelson, Phys. Rev. B **50**, 8996 (1994).

[15] O. Albert, M. Duijser, J. C. Loulergue, and J. Etchepare, J. Opt. Soc. Am. B (to be published).

[16] D. P. Kien, J. C. Loulergue, and J. Etchepare, Opt. Commun. **101**, 53 (1993).

[17] Crystals kindly supplied by K. Wojcik, Institute of Physics, 40007 Katowice, Poland.

[18] S. Singh, J. P. Remeika, and J. R. Potopowicz, Appl. Phys. Lett. **20**, 135 (1972).

[19] A. S. Barker and R. Loudon, Rev. Mod. Phys. **44**, 18 (1972).

[20] P. Bourson and M. Fontana (private communication).

[21] P. C. M. Planken, Dr. thesis, University Amsterdam, 1991.

[22] Y. Okamoto, P. Wang, and J. F. Scott, Phys. Rev. B **32**, 6787 (1985).

[23] J. P. Sokholov, L. L. Chase, and D. Rytz, Phys. Rev. B **38**, 597 (1988).